

Taming Client Dropout and Improving Efficiency for Distributed Differential Privacy in Federated Learning

Zhifeng Jiang
HKUST

Wei Wang
HKUST

Ruichuan Chen
Nokia Bell Labs

Abstract

Federated learning (FL) is increasingly deployed among multiple clients (e.g., mobile devices) to train a shared model over decentralized data. To address the privacy concerns, FL systems need to protect the clients’ data from being revealed during training, and also control the data leakage through trained models when exposed to untrusted domains. Distributed differential privacy (DP) offers an appealing solution in this regard as it achieves an informed tradeoff between privacy and utility without a trusted server. However, existing distributed DP mechanisms work impractically in the presence of *client dropout*, resulting in either poor privacy guarantees or degraded training accuracy. In addition, these mechanisms also suffer from severe efficiency issues with long time-to-accuracy training performance.

We present Hyades, a distributed differentially private FL framework that is highly efficient and resilient to client dropout. Specifically, we develop a novel ‘add-then-remove’ scheme where a required noise level can be enforced in each FL training round even though some sampled clients may drop out in the end; therefore, the privacy budget is consumed carefully even in the presence of client dropout. To boost performance, Hyades runs as a distributed pipeline architecture via encapsulating the communication and computation operations into stages. It automatically divides the global model aggregation into several chunk-aggregation tasks and pipelines them for optimal speedup. Evaluation through large-scale cloud deployment shows that Hyades can efficiently handle client dropout in various realistic FL scenarios, attaining the optimal privacy-utility tradeoff and accelerating the training by up to $2.1\times$ compared to existing solutions.

1 Introduction

Federated learning (FL) [47, 56] allows multiple clients (e.g., mobile and edge devices) to collaboratively train a shared model under the orchestration of a central server. In scenarios where the number of clients is large (e.g., millions of mobile

devices), the server dynamically *samples* a small subset of clients to participate in each training round [18]. The sampled clients download the global model from the server, compute individual local updates using private data, and upload local updates to the server for global aggregation. Throughout the training, no client’s data is exposed directly. FL has been deployed in various domains to enable a multitude of privacy-sensitive AI applications [36, 54, 55, 62, 64, 84].

However, only keeping client data on device is insufficient to preserve data privacy. Recent work shows that sensitive data can still be revealed through message exchanges in FL training [30, 31, 37, 58, 83, 87]. It is also possible, with theoretical and empirical evidences, to infer client’s data from the trained models by leveraging their information memorization capability [21, 61, 74, 78, 86].

Current FL systems often use *differential privacy* (DP) [33] to perturb the aggregate model update in each training round, so as to bound the leakage of individual clients’ data throughout training. Among the three typical DP models (i.e., central [57, 68], local [66], and distributed DP [11, 45, 79]), the *distributed DP* is the most appealing DP model in the FL setting as it: 1) assumes *no trusted server* (as opposed to central DP), and 2) imposes *minimum noise* given a privacy budget (as opposed to local DP), causing little utility loss to the trained models. Specifically, given a global privacy budget that should not be exceeded, the system first computes the minimum random noise required in each training round to control data leakage. Afterward, in each round, every sampled client adds a small portion of the required noise to its local update. Together, the aggregate update at the server is perturbed by *exactly* the minimum required noise. In distributed DP, local updates are aggregated using the secure aggregation (SecAgg) protocol [19], which ensures that the (untrusted) server learns no individual updates but the aggregate result.

Existing distributed DP mechanisms, however, face two practical challenges when deployed in real-world FL systems. First, the privacy guarantee of distributed DP can be compromised in the presence of *client dropout*, which can occur anytime, for instance, due to network errors, low battery, or

changes in eligibility, as observed in production [18, 51, 85]. For these dropped clients, their noise contributions are missing in the aggregate update, leading to insufficient DP protection and thus consuming more privacy budget than originally planned in each round [45]. As the privacy budget runs out quickly, the training has to stop early, resulting in a significant model utility loss (§2.3).

Second, in addition to the privacy issue caused by client dropout, the use of SecAgg protocol [19] in distributed DP raises severe efficiency issues. This is because, to ensure secure aggregation, SecAgg performs multi-round communications and heavy cryptographic computations. The overhead of these operations grows quadratically with the number of sampled clients, significantly limiting the scalability of its deployment in practice [18]. In our experiments, SecAgg can take up to 91% of the training time (§2.3). Thus, it is critical to accelerate SecAgg for distributed DP in the FL scenario.

In this paper, we present Hyades, an efficient FL framework that enables dropout-resilient distributed DP in FL. Hyades addresses both the privacy and efficiency issues of distributed DP in an FL system with two key contributions. First, to ensure that the aggregate model update is perturbed with exactly the minimum required noise regardless of client dropout after being sampled, we devise a novel *add-then-remove* scheme (§4). Specifically, Hyades first lets each sampled client add excessive noise to its local update, such that the aggregate noise retains sufficient even if many sampled clients drop out in the end. After aggregation, the server removes part of the excessive noise that is over the minimum noise requirement, based on the actual client participation. Using Shamir’s secret sharing [73], we ensure that the entire scheme is dropout-resilient. In addition, we devise an efficient *approximate* noise enforcement scheme to further reduce the complexity of computation and communication without a noticeable utility loss.

Second, to accelerate SecAgg used in distributed DP, we run Hyades as a *distributed parallel architecture* that encapsulates computation- and communication-intensive operations (e.g., data encoding and transmission) in SecAgg into pipeline stages (§5). Specifically, it optimally divides a client’s update into multiple chunks, and schedules chunk-aggregation tasks in parallel for maximum acceleration. As our approach targets system-level optimizations, it is general and can be used to accelerate other secure aggregation protocols (e.g., [44, 76, 77]) in distributed DP, for which we also provide a generic programming interface in Hyades (§6).

We implemented Hyades and evaluated its performance with various FL training tasks in a 100-node EC2 cluster that emulates the hardware heterogeneity of client devices (§7). Evaluation results show that the required noise being added to an aggregate model update in Hyades can always be enforced under various client dropout dynamics, while still preserving the model utility. In terms of the end-to-end performance, Hyades’s pipeline execution speeds up the baseline system by up to $2.1\times$, without impairing other desirable properties

such as dropout resilience. The entire codebase of Hyades is open-sourced at [3].

2 Background and Motivation

2.1 Federated Learning and Threat Model

Federated Learning. Federated learning (FL) enables a large number of clients (e.g., millions of mobile and edge devices) to collaboratively build a global model without sharing local data [47, 56]. In FL, a (logically) centralized server maintains the global model and orchestrates the iterative training. At the beginning of each training round, the server randomly samples a subset of available clients as participants [18].¹ The sampled clients perform local training to the downloaded global model using their individual private data and report only the model updates to the server. The server collects the updates from participants until a certain deadline, and aggregates these updates. It then uses the aggregate update (e.g., FedAvg [56]) to refine the global model.

Threat Model. Although client data is not directly exposed in the FL process, a large body of research has shown that it is still possible to reveal sensitive client data from individual updates or trained models via *data reconstruction* or *membership inference* attacks [21, 30, 31, 37, 58, 61, 65, 74, 78, 83, 86, 87]. For example, an adversary can accurately reconstruct a client’s training data from its gradient updates [58, 65, 87]; an adversary can also infer from a trained language model whether a client’s private text is in the training set [21, 78]. We aim to defend against both data reconstruction and membership inference attacks by controlling the exposure of individual clients’ data in the training process.

We assume that both the centralized server and the sampled clients are *honest but curious*. They faithfully follow the specified training process; while doing so, they are eager to pry on the others’ data by means of membership or reconstruction attacks. We do not assume collusion between the server and clients, or among clients themselves. Nevertheless, it is worth mentioning that our work can be easily extended to provide the same privacy guarantee with negligible extra utility loss when the collusion is “mild” (which is typically the case in reality). We will discuss this extension in §8.

2.2 Differential Privacy

Differential privacy (DP) [28, 32, 33] is known to effectively address the reconstruction and membership attacks in our threat model. In a nutshell, these two classes of attacks work by finding data entries that make the observed messages (e.g., local updates and their aggregates) more likely. To prevent these attacks, DP ensures that no specific data entry (or more

¹Many recent studies suggest using more advanced sampling algorithms in FL to improve the time-to-accuracy performance [22, 42, 48, 52].

strongly in FL, client participation) can noticeably increase the likelihood of such observed messages. This guarantee is captured by two parameters, ϵ and δ [33]. Given any neighboring training sets D and D' that differ only in the inclusion of a single client's data, the aggregation procedure f is (ϵ, δ) -differentially private if, for any set of output R , we have

$$\Pr[f(D) \in R] \leq e^\epsilon \cdot \Pr[f(D') \in R] + \delta. \quad (1)$$

In other words, a change in a client's participation yields at most a multiplicative change of e^ϵ in the probability of any output, except with a probability δ . Intuitively, smaller ϵ and δ indicate a stronger privacy guarantee.

A key property of DP is composition which states that the process of running (ϵ_1, δ_1) -DP and (ϵ_2, δ_2) -DP computations on the same dataset is $(\epsilon_1 + \epsilon_2, \delta_1 + \delta_2)$ -DP. This allows one to account for the privacy loss resulting from a sequence of DP-computed outputs, such as the release of multiple aggregate updates in FL. Tighter analysis of cumulative privacy loss can be achieved with Rényi DP [60].

Central DP and Local DP. One way to apply DP in FL is to let the server add DP-compliant noise to the aggregate update, i.e., the *central DP* scheme [47]. However, the server must be trusted as it has access to the (unprotected) aggregate update. While the server may establish a trusted execution environment (TEE) [13, 40] with hardware support, it is still vulnerable to various attacks, e.g., side-channel attacks [24, 81]. An alternative DP scheme is *local DP*, in which each sampled client adds DP noise to perturb its local update before contacting the server. As long as the noise added by a client is sufficient for a DP guarantee on its own, its privacy is preserved regardless of the behavior of other clients or the server. This, however, results in excessive accumulated noise in the aggregate update, significantly harming the model utility [45].

Distributed DP. Compared to central and local DP, *distributed DP* offers an appealing solution in FL scenarios as it: 1) requires no trusted server, and 2) imposes minimum noise given a privacy budget. This is achieved by simulating a trusted third party via cryptographic protocols. In distributed DP, a privacy goal is specified as a global privacy budget (ϵ_G, δ_G) , which can be viewed as a non-replenishable resource that is consumed by each release of an aggregate update. Ideally, by the time when the training completes, the remaining privacy budget should be zero, so as to meet the privacy goal at the expense of minimum DP noise and model utility loss. This requires the system to perform *offline noise planning* ahead of time to determine the minimum required noise that should be added to the aggregate update in each training round to control the privacy loss.

The system then proceeds to *online noise enforcement*. In each training round, it evenly splits the noise adding task to all sampled clients. Each of them slightly perturbs its update by adding an even share of the minimum required noise. The clients then mask their updates and send them to the server

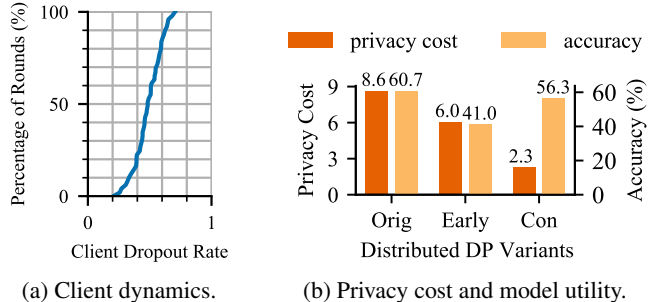


Figure 1: Privacy impact of client dropout.

using the secure aggregation (SecAgg) protocol [19], which ensures that the server learns nothing but the aggregate update that is perturbed with exactly the minimum required noise. Note that, besides the commonly-used SecAgg, the distributed DP can also be implemented using alternative approaches (e.g., secure shuffling [17, 25, 34]). In this paper, we focus on the approaches using SecAgg, given their popularity in FL.

2.3 Practical Issues of Distributed DP

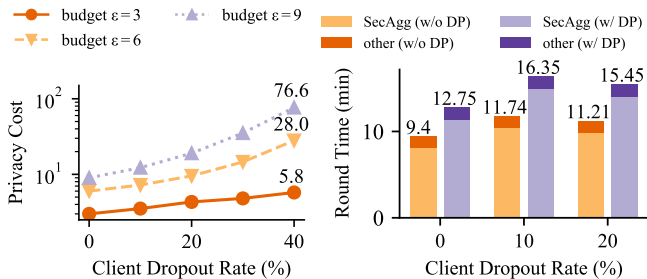
While distributed DP can achieve an appealing privacy-utility tradeoff, its deployment in real world has significant issues.

2.3.1 Privacy Issue Caused by Client Dropout

In FL training, *client dropout* can occur anytime, e.g., due to low battery, poor connection, network error, or switching to a metered network. The prevalence of client dropout, which has been widely observed in real-world systems [18, 51, 85], raises a severe privacy issue in distributed DP. Specifically, if clients drop out after being sampled, without their noise contributions, the total noise added to the aggregate update falls below the minimum required level. This leads to increased data exposure that forces the system to consume more privacy budget than originally planned for each round. Should the system follow the original FL training plan (e.g., completing the training after a certain number of rounds), the cumulative privacy loss inevitably exceeds the global privacy budget [45].

To illustrate this issue, we analyze the potential impact of client dropout in a realistic FL task. Specifically, we run an FL testbed in which 100 clients jointly train a ResNet-18 [9] model over the CIFAR-10 dataset [49] for 150 rounds.² To emulate the dynamics of clients, we use a large-scale user behavior dataset spanning 136k mobile devices [85] and extract 100 volatile users. We sample 16 clients to train in each round and observe great dynamics in their availability, as shown in Figure 1a: 1) each training round has at least 20% of the sampled clients dropped out, and 2) nearly half of the rounds have over 50% of the sampled clients dropped out. In this case, the original distributed DP training with a global privacy

²Detailed cluster and training settings are given in §7.1.



(a) Privacy impact under various client dropout rates. (b) Runtime breakdown of one training round.

Figure 2: Impact of client dropout rates on privacy cost and training efficiency. Detailed cluster settings are given in §7.1.

budget $\epsilon_G = 6$ ends up consuming an ϵ of 8.6 at the 150th round due to the missing noise from the dropped clients (see Orig in Figure 1b).

Naive Solutions and Limitations. One solution to this issue is to stop the training early when the privacy budget runs out. However, this inevitably harms the model utility. In the aforementioned example, the early-stop solution has to stop at the 86th round, reducing the model utility by over 29% (see Early in Figure 1b) compared to the non-private training (Orig). Another solution is to make a conservative estimation on the per-round dropout rate (e.g., 80%) during offline noise planning. However, this leads to suboptimal model utility (see Con in Figure 1b) due to the excessive noise added when client dropout is often less severe than the conservative estimation.

Client Dropout Rate. To further capture the relationship between privacy violation and dropout severity, we let the clients randomly drop with a configurable rate after being sampled. Figure 2a shows the final achieved privacy guarantee when the above training task completes in 150 rounds with dropout rates varying from 0% to 40%, under three privacy budgets. As the dropout rate increases, more clients’ data gets exposed during training, leading to a larger privacy cost (i.e., larger deficit beyond the target privacy budget).

2.3.2 Performance Issue Caused by Secure Aggregation

Beside the privacy issue caused by client dropout, the SecAgg algorithm [19] used in distributed DP creates a severe performance issue. Specifically, to ensure the server learns no individual update from any client but the aggregate update only, SecAgg lets clients synchronize secret keys and use them to generate zero-sum masks. This involves extensive use of pairwise masking and secret sharing, incurring high complexity in both computation and communication (Appendix A).

To quantify the performance impact of SecAgg, we refer to Figure 2b which shows the breakdown of the average runtime of one training round in the previous experiment with varying dropout rates. For comparison, we also run the experiment

with SecAgg but add no DP noise to the aggregate update. In all experiments with and without DP, the cost of SecAgg dominates across various client dropout rates, accounting for 86-91% of the training time in each round.

Existing Solutions and Limitations. There have been active studies on improving the performance of secure aggregation, but they all have significant limitations. For example, one guarantee provided by SecAgg is to ensure that the aggregate update can be correctly computed and decoded under any random dropout, provided that the number of dropped clients does not exceed a specified threshold. However, recent secure aggregation protocols such as SecAgg+ [16], CCESA [26], FastSecAgg [44], and TurboAgg [76] all relax this guarantee into a probabilistic one, i.e., the desired aggregated model may not be recovered with some probability [77]. Although this may not be a problem for LightSecAgg [77], its communication complexity varies depending on the number of surviving clients (U in the paper) in a round. If U approaches the collusion tolerance (T in the paper), the cost can become much more prohibitive than that of SecAgg.

3 Hyades Overview

We design Hyades, an efficient FL framework that enables dropout-resilient distributed DP. We first give an overview of Hyades, including its design goals and system architecture.

Design Goals. Hyades aims to achieve two design goals that address the aforementioned privacy and performance issues of distributed DP in FL.

1) *Resilience to client dropout:* In each training round, the system should ensure that the minimum required noise is added to the aggregate update, regardless of client dropout after being sampled. Given the dynamics of client availability, however, it is hard to predict such client dropout rate and to instruct the sampled clients to add just enough noise shares at the moment of client sampling. Consequently, Hyades first makes a conservative estimation on the dropout severity, and then lets each client add excessive noise to its local update to tolerate dropout even in the worst case. Next, to avoid degrading the final model utility, Hyades removes part of the excessive noise that is over the minimum requirement from the aggregated update based on the actual client participation.

To instantiate the above idea, we face two key challenges: a) *Robustness:* clients can drop out anytime, not only during the secure aggregation of perturbed local updates but also during the process of excessive noise removal. To completely handle client dropout, the noise removal itself should also be dropout-resilient. b) *Efficiency:* the extra time and bandwidth costs incurred should be minimal. Hyades addresses both challenges with a novel ‘add-then-remove’ protocol and its efficient approximation (§4).

2) *High efficiency of secure aggregation:* Given the high complexity of SecAgg and its dominance in training time, the

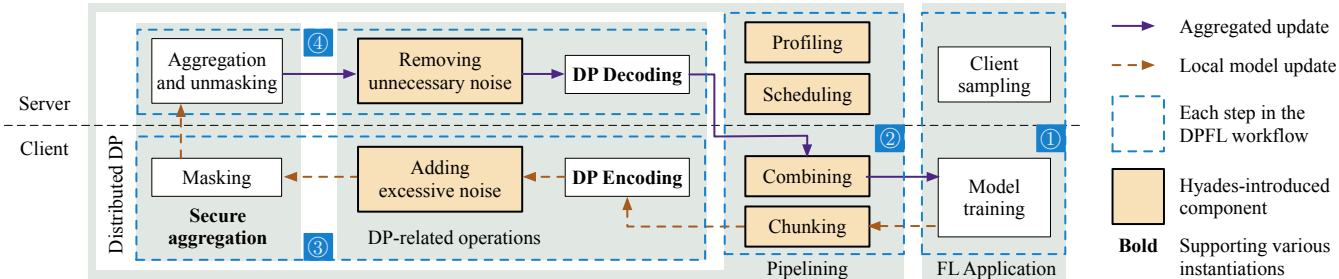


Figure 3: An overview of Hyades’ system architecture and how it fits in the existing FL workflow.

system should optimize the SecAgg operations to mitigate the performance bottleneck. Hyades targets system-level optimizations which preserve all the existing merits of using SecAgg. Given the variation of dominant resources over time in SecAgg, we design a systematic scheme to pipeline the use of different resources. In particular, Hyades adopts a generic distributed parallel architecture that optimally partitions the local update from a client into chunks and automatically coordinates their processing by overlapping computation and communication for maximum acceleration (§5).

System Architecture. For easy adoption and high applicability, Hyades is designed to be complementary to existing differentially private FL (DPFL) frameworks. Figure 3 shows how Hyades fits in the existing DPFL workflow, with yellow boxes being Hyades-introduced components. ① *Client sampling and training*: at the beginning of each round, the server randomly samples a subset of available clients as participants. The sampled clients then fetch the global model from the server and compute local updates using their individual private data. ② *Pipeline preparation*: for each participant, the server profiles its processing speed and comes up with an optimal pipeline execution plan. Following the plan, the client chunks the local update for pipelined aggregation. ③ *Client processing*: for each update chunk, the client perturbs it with the standard DP encoding scheme and our ‘add-then-remove’ noise enforcement approach. The perturbed chunk is further masked following the SecAgg protocol. ④ *Server-side aggregation*: the server aggregates and un.masks the received update chunks and also removes the excessive parts of their DP noises to ensure that the residual noise stays at the minimum required level. The server then uses each aggregated update chunk to refine the respective part of the global model.

4 Dropout-Resilient Noise Enforcement

We first formalize the noise enforcement problem under client dropout, and present the technical intuition to address this problem (§4.1). We then describe a novel ‘add-then-remove’ noise enforcement approach that realizes this intuition (§4.2), as well as describe its efficient approximation (§4.3).

4.1 Technical Intuition

Without loss of generality, we assume that the random noise distribution $\chi(\sigma^2)$ used in DP is *closed under summation* with respect to the variance σ^2 . That is, given two noises $X_1 \sim \chi(\sigma_1^2)$ and $X_2 \sim \chi(\sigma_2^2)$, where X_1 and X_2 are independent, we have $X_1 \pm X_2 \sim \chi(\sigma_1^2 + \sigma_2^2)$. For example, both Gaussian and Skellam [11] distributions exhibit this property.

We start with a formal description of the original noise addition process used in distributed DP, denoted as *Orig*.

Definition 1 (*Orig*). *Given the set of sampled clients S and the target noise level σ_*^2 in a certain round, *Orig* lets each client $c_j \in S$ perturb its update Δ_j by adding noise $n_j \sim \chi(\sigma_*^2/|S|)$ and upload the result $\tilde{\Delta}_j = \Delta_j + n_j$ to the server for aggregation.*

In *Orig*, all sampled clients collaboratively add enough noise. However, as described in §2.3.1, its problem is that when some clients drop after being sampled, their noise contributions are missing; thus, the eventual noise aggregated at the server will be insufficient. One potential fix is to let the server add back the missing noise contributed by the dropped clients [45]. However, this is not viable under our threat model as the curious server has access to the insufficiently perturbed aggregate result and can infer clients’ data from it (§2.1).

Add-Then-Remove Noise Enforcement. To ensure that the aggregate noise never goes inefficient and always lands at the minimum required level, we design an ‘add-then-remove’ noise enforcement scheme: 1) each sampled client first adds a higher-than-required amount of noise to its model update, rendering an overly perturbed aggregate update despite client dropout, and 2) the server removes the excessive part of the aggregate noise based on actual dropout outcome. This noise enforcement can be realized by two possible approaches:

- *Strawman*: During noise addition, each sampled client adds its noise share n_o to the local update, and sends the noisy update as a whole to the server. To facilitate noise removal, each surviving client computes the newly-required noise n_u based on actual client dropout outcome, and subtracts the original noise share n_o . To ensure that

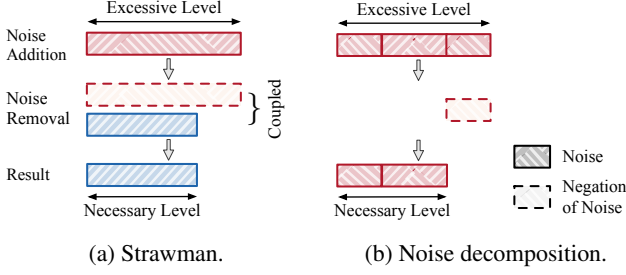


Figure 4: Two ‘add-then-remove’ approaches.

the noise removal is privacy-preserving, only ‘ $n_u - n_o$ ’ is transmitted to the server and added to the aggregate update (Figure 4a). This approach was adopted by [14].

- *Noise Decomposition*: Instead of adding noise as a whole, each sampled client decomposes its noise share into multiple additive components that can be added separately to the client’s local update. For privacy-preserving noise removal, each surviving client only sends the noise components that are over the newly-required noise amount to the server for them to be subtracted from the aggregate update (Figure 4b).

Comparison. One difference between the two approaches lies in their *efficiency*. In FL, a DP noise is a sequence of pseudo-random numbers (PRNs) of the same length (e.g., millions to billions) as the model, and can be uniquely generated via feeding a seed (e.g., 20 bytes) into a secure PRN generator. Therefore, during noise removal, the ‘noise decomposition’ approach can let each surviving client send the corresponding seeds to the server for it to generate each noise component that needs to be subtracted. However, in the ‘strawman’ approach, each surviving client has to generate and send the updated noise $n_u - n_o$ as a whole to hide the two individual noises; otherwise, the server can use them to reconstruct the noise-free aggregate update. This leads to poor efficiency as the communication cost of noise removal in ‘strawman’ prohibitively increases with the ever-growing model size.

Another difference lies in their *robustness*. This is because, in reality, surviving clients can also drop out in the middle of noise removal. Missing their noise updates, the server cannot fully remove the excessive noise added to the aggregate update. To tackle this issue, the ‘noise decomposition’ approach can efficiently back up each noise component before model aggregation by secret-sharing its seed across clients (e.g., via the Shamir’s scheme [73]). Such a scheme, however, does not apply to ‘strawman’ as the updated noise to transmit can neither be generated with a seed nor determined before model aggregation.

4.2 Add-Then-Remove with Noise Decomposition

Due to the poor efficiency and robustness of the ‘strawman’ approach, we opt to instantiate the ‘add-then-remove’ noise enforcement scheme with ‘noise decomposition’. Specifically, there are two technical challenges in its design:

- **C1**: Given various dropout outcomes of a training round, how to decompose a client’s noise share to accommodate every possible requirement during noise removal?
- **C2**: Transmitting seeds instead of noise can reduce network footprint, but how to secret-share them before secure aggregation to enable dropout-resilient noise removal?

Noise Addition and Removal. To tackle the challenge **C1**, we start with how much noise a sampled client should add. Without loss of generality, we assume that the system’s *tolerance* to client dropout is a configurable parameter specified by the FL developer. Let S be the set of sampled clients in a certain training round, among which the system can tolerate up to t dropouts. Let σ_*^2 be the target noise level in each round. To meet this noise level even in the worst case, each client in our Hyades system adds an excessive noise at the level of $\frac{\sigma_*^2}{|S|-t}$. In doing so, even if there are t clients dropped after being sampled, the total noise contributed by the surviving $|S| - t$ clients is still sufficient at the target level.

We next derive how much noise a surviving client should help the server to remove based on the actual dropout outcome. When there are fewer than t clients dropped after being sampled, the aggregate noise at the server exceeds the target level; thus, part of the excessive noise needs to be removed for model utility. Let D denote the set of clients dropped after being sampled, where $D \subset S$ and $|D| \leq t$. The amount of excessive noise that should be removed by the server is:

$$l_{\text{ex}} = \underbrace{(|S| - |D|)}_{\text{Actual noise level}} \frac{\sigma_*^2}{|S| - t} - \sigma_*^2 = \frac{t - |D|}{|S| - t} \sigma_*^2. \quad (2)$$

Hyades evenly distributes the noise removal task across surviving clients, therefore, each of them needs to help the server remove the noise of level:

$$l'_{\text{ex}} = \frac{l_{\text{ex}}}{|S| - |D|} = \sigma_*^2 \left(\frac{1}{|S| - t} - \frac{1}{|S| - |D|} \right). \quad (3)$$

Noise Decomposition for Precise Control. Equation (3) indicates that the noise to be removed by a surviving client decreases when the number of dropped clients increases, and vice versa. Given this monotonicity, each client in Hyades can carefully decompose its added noise share into multiple additive components, and remove some of such noise components when needed for the precise control of noise level.

As a concrete example, consider a scenario where the number of sampled clients $|S| = 4$, the dropout tolerance $t = 2$,

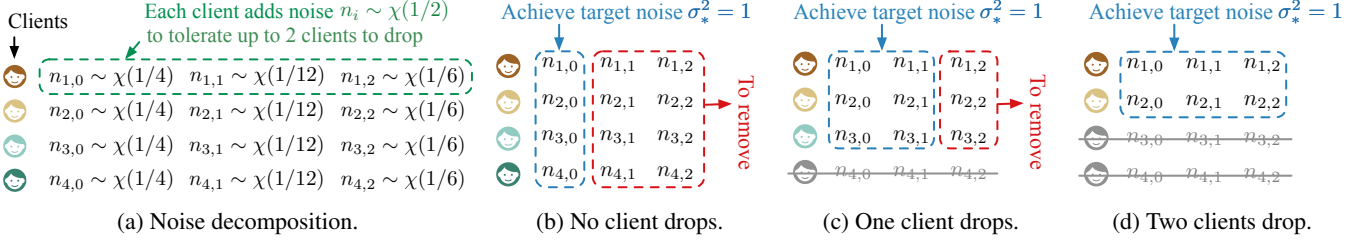


Figure 5: An example illustrating the ‘add-then-remove’ approach with noise decomposition, and how it can deal with client dropout precisely.

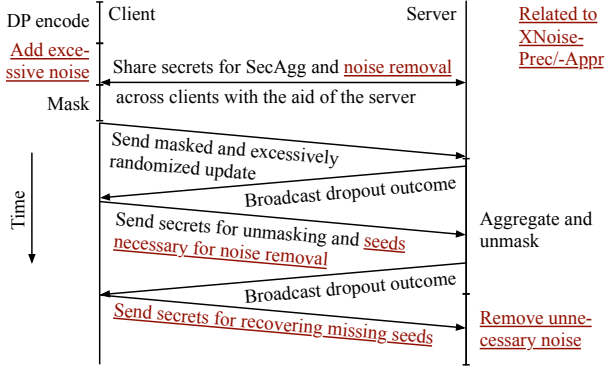


Figure 6: XNoise-Prec/-Appr fits well into the existing workflow of distributed DP with SecAgg in FL.

and the target noise level $\sigma_*^2 = 1$. To enforce this target noise level even if 2 clients drop out, the noise added to each client’s update should be of the level 1/2. Furthermore, as shown in Figure 5a, such a noise can be added as 3 separate components of level 1/4, 1/12, and 1/6, respectively, then one can accommodate all possible dropout outcomes within the tolerance by subtracting a subset of the added components to precisely remove the excessive noise. For example, if no client drops, i.e., $|D| = 0$, each surviving client removes $l'_{ex} = 1/12 + 1/6$ (Figure 5b); if one client drops, i.e., $|D| = 1$, each surviving client removes $l'_{ex} = 1/6$ (Figure 5c); if two clients drop, i.e., $|D| = 2$, each surviving client removes $l'_{ex} = 0$ (Figure 5d).

To be general, Hyades lets each client $c_i \in S$ decompose the added noise $n_i \sim \chi(\frac{\sigma_*^2}{|S|-t})$ into $t + 1$ components, i.e., $n_i = \sum_{k=0}^t n_{i,k}$ where $n_{i,0} \sim \chi(\frac{\sigma_*^2}{|S|})$ and $n_{i,k} \sim \chi(\frac{\sigma_*^2}{(|S|-k+1)(|S|-k)})$ for $k = 1, 2, \dots, t$. These noise components are constructed in a way such that when there are $|D|$ clients dropped after being sampled, the noise components $n_{i,k}$ contributed by the surviving clients $c_i \in S \setminus D$ with the index $k > |D|$ become excessive and should be removed by the server. One can verify that the aggregate of these removed components is exactly l_{ex} , i.e., $\sum_{c_i \in S \setminus D} \sum_{k=|D|+1}^t n_{i,k} \sim \chi(l_{ex})$. We formalize the noise enforcement process for precise noise control as XNoise-Prec.

Definition 2 (XNoise-Prec). In each training round, a sam-

pled client $c_i \in S$ adds the intended excessive noise to its update Δ_i and sends the perturbed result $\tilde{\Delta}_i = \Delta_i + \sum_{k=0}^t n_{i,k}$ to the server. Among these sampled clients, a subset D have dropped where $|D| \leq t$. The server calculates the aggregate update $\tilde{\Delta} = \sum_{c_i \in S \setminus D} \tilde{\Delta}_i$, and then removes some excessive noise components contributed by the surviving clients (known as survivors) to precisely enforce the target noise level, i.e., $\tilde{\Delta} - \sum_{c_i \in S \setminus D} \sum_{k=|D|+1}^t n_{i,k}$.

Note that, as described in §4.1, Hyades allows clients to transmit the seeds that are used to generate the requested noise components instead of those components. As the size of a seed is only a few bytes and does not grow with large models, this greatly reduces the communication overhead.

Secret Sharing for Dropout-Resilient Noise Removal. To address the challenge C2, Hyades uses Shamir’s secret sharing scheme [73] for seed bookkeeping: each sampled client secretly shares with others the seeds it uses to generate local noise components before the secure aggregation takes place. As such, to recover a local noise component during noise removal, the server first directly consults the related client on the corresponding seed. If the client drops out before reporting the seed, the server then initiates one additional communication round to collect the secret shares of the seed from all available clients. The server can recover the seed provided that the number of responding clients in this communication round exceeds a certain threshold specified by the secret sharing scheme [73].

Putting Them All Together. Figure 6 illustrates how our precise noise enforcement XNoise-Prec fits in the existing workflow of distributed DP in FL. We summarize the complexity of computation and communication of XNoise-Prec for both the server and a client in Table 1. The complexity analysis is given in Appendix B. As for the privacy guarantee, XNoise-Prec strictly enforces the target noise level, as established by Theorem 1. The proof is given in Appendix C.

Theorem 1. XNoise-Prec ensures the noise level in the aggregate update is exactly σ_*^2 , regardless of client dropout.

Table 1: The computational and communication complexity of XNoise-Prec/-Appr, where $|S|$ is the number of sampled clients, and d is the model size measured by the number of model parameters.

Protocol		XNoise-Prec	XNoise-Appr
Comp.	Client	$O(d S + S ^3)$	$O(d \log S + S ^2 \log S)$
	Server	$O(d S ^2 + S ^3)$	$O(d S \log S + S ^2 \log S)$
Comm.	Client	$O(S ^2)$	$O(S \log S)$
	Server	$O(S ^3)$	$O(S ^2 \log S)$

4.3 Trading Precision for Scalability

While XNoise-Prec ensures precise noise enforcement at the target level, its complexity (Table 1) may limit its scalability when a large number of clients are sampled as participants. We therefore devise an efficient noise control scheme XNoise-Appr that relaxes the requirement of precise noise enforcement for improved scalability (while privacy is still guaranteed). Our insight is that the model utility should not have a noticeable degradation when the added noise is only slightly higher than the target level, thanks to machine learning’s error-tolerant nature [67].

We use the same notation as in §4.2. In XNoise-Appr, each sampled client $c_i \in S$ approximates the intended excessive noise $n_i \sim \chi(\frac{\sigma_*^2}{|S|-t})$ using only $\lceil \log_2 t \rceil + 2$ noise components (as opposed to Xnoise-Prec which decomposes n_i into $t + 1$ components). These noise components are carefully designed as a geometric series with ratio $1/2$. After computing the aggregate update, the server removes certain noise components of the surviving clients, so as to approximately maintain the residual noise at or slightly above the target level. Compared to the precise scheme, this approximate scheme deals with a significantly smaller number of noise components (i.e., $O(\log |S|)$ for each client in XNoise-Appr as compared with $O(|S|)$ in Xnoise-Prec), making it much more efficient (see Table 1). We formalize the process of XNoise-Appr below.

Definition 3 (XNoise-Appr). Let $\tau = \lceil \log_2 t \rceil$ and $\eta = \frac{\sigma_*^2 t}{2^\tau |S| (|S|-t)}$. Each client $c_i \in S$ perturbs its update Δ_i by adding $\tau + 2$ noise components, i.e., $\tilde{\Delta}_i = \Delta_i + \sum_{k=0}^{\tau+1} n_{i,k}$, where $n_{i,0} \sim \chi(\sigma_*^2/|S|)$, $n_{i,1} \sim \chi(\eta)$, and $n_{i,k} \sim \chi(\eta \cdot 2^{k-2})$ for $k = 2, \dots, \tau + 1$. The perturbed update $\tilde{\Delta}_i$ is then sent to the server for aggregation.

After calculating the aggregated update $\tilde{\Delta} = \sum_{c_i \in S \setminus D} \tilde{\Delta}_i$, the server removes from it a subset of noise components contributed by the surviving clients. Specifically, when there is no dropout ($D = \emptyset$), the server removes all $n_{i,k}$ where $k > 0$; otherwise, for each surviving client $c_i \in S \setminus D$, the server removes $n_{i,k}$ where $k \geq 2$ and $b_{k-1} = 1$. Here, $[b_\tau, b_{\tau-1}, \dots, b_1]$ is the τ -bit binary representation of the integer $\lfloor \lambda/\eta \rfloor$, where b_τ is the most significant bit and $\lambda = \frac{(t-|D|)\sigma_*^2}{(|S|-t)(|S|-|D|)}$.

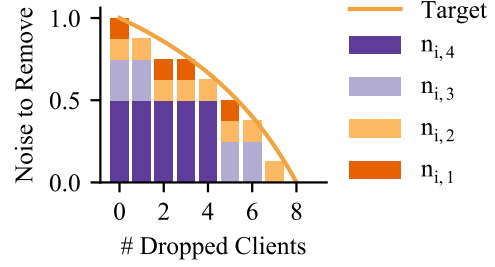


Figure 7: XNoise-Appr trades precision for scalability via a geometric series of noise components.

As a concrete example, consider a scenario where there are 16 sampled clients, the dropout tolerance is 8, and the target noise level in the aggregate update is 16. Besides the basic noise component $n_{i,0} \sim \chi(2)$, a client i only needs to add 4 excessive noise components: $n_{i,1} \sim \chi(1/8)$, $n_{i,2} \sim \chi(1/8)$, $n_{i,3} \sim \chi(1/4)$, and $n_{i,4} \sim \chi(1/2)$. Moreover, as shown in Figure 7, during noise removal, a surviving client i only needs to help the server remove at most 4 noise components despite client dropout. Note that, the noise to remove approximates but never exceeds the target level (yellow line).

The following theorem further bounds the gap between the target noise level and the one achieved by the XNoise-Appr approximation. The proof is given in Appendix C.

Theorem 2. Given the target noise level σ_*^2 , XNoise-Appr ensures that the approximate noise is within $[\sigma_*^2, \sigma_*^2 + \frac{\sigma_*^2}{|S|-t}]$.

There are two takeaways from Theorem 2. First, the noise imposed by XNoise-Appr is never less than the target level, thus controlling the data leakage within the privacy budget. Second, the extra noise added by XNoise-Appr is rather small compared to the target noise, within a factor of $\frac{1}{|S|-t} \approx \frac{1}{|S|}$. As the number of sampled clients increases (i.e., larger $|S|$), XNoise-Appr gives a more accurate approximation, and its speedup over XNoise-prec becomes more significant (Table 1). In our experiments, XNoise-Appr indeed causes a negligible accuracy loss as compared to XNoise-prec (§7.2).

5 Optimal Pipeline Acceleration

As described in §2.3.2, the secure aggregation protocol (e.g., SecAgg [19]) used for distributed DP in FL creates a severe performance bottleneck and dominates the total training time in each round. In addition, the integration with our dropout-resilient noise enforcement scheme may further add to its inefficiency. In this section, we devise a distributed parallel architecture that enables pipeline parallelism for SecAgg via the optimal pipeline scheduling of computation and communication operations at both the server and clients (§5.1 and §5.2). The compatibility of our distributed parallel architecture with the distributed DP is achieved by a DP-compliant

Table 2: Partitioning the workflow of dropout-resilient distributed DP into multiple stages for pipelined execution.

Step	Operation	Stage (Resource)
1	Clients encode updates.	
2	Clients generate security keys.	
3	Clients establish shared secrets.	1 (c-comp)
4	Clients mask encoded updates.	
5	Clients upload masked updates.	2 (comm)
6	Server deals with dropout.	
7	Server computes aggregate update.	3 (s-comp)
8	Server updates the global model.	
9	Server dispatches the aggregate.	4 (comm)
10	Clients decode the aggregate.	
11	Clients use the aggregate.	5 (c-comp)

update clipping scheme (§5.3). While we base our design on SecAgg, our approach is general and can be used to accelerate other secure aggregation protocols in distributed DP.

5.1 Staging Workflow for Pipelined Execution

We identify three types of operations in distributed DP that use different system resources and can be pipelined: 1) s-comp that uses the compute resources (e.g., CPU, GPU, and memory) of the server, 2) c-comp that uses the compute resources of clients, and 3) comm that facilitates server-client communications. Given a distributed DP algorithm and its workflow consisting of a sequence of operations, we group consecutive operations that use the same system resource into a *stage*. As shown in Table 2, the workflow of our distributed DP algorithm using SecAgg can be partitioned into 5 stages for pipelined execution in Hyades. Note that workflow staging is not limited to a particular algorithm, but generally applies to distributed DP using various secure aggregation protocols.

5.2 Pipeline-Parallel Aggregation

Hyades enables *pipeline parallelism* to accelerate the aggregation workflow. It evenly partitions each client’s update Δ_i into m chunks $\Delta_{i,1}, \dots, \Delta_{i,m}$. This divides the global update aggregation into m chunk-aggregation tasks, where the j -th task aggregates the j -th chunks of all clients, i.e., $\sum_i \Delta_i = (\sum_i \Delta_{i,1}) \# \dots \# (\sum_i \Delta_{i,m})$, where $\#$ denotes concatenation. Each chunk-aggregation task follows the same processing stages as in the global aggregation workflow (Table 2). Given that there are m chunk-aggregation tasks, Hyades pipeline-schedules their processing stages to optimally overlap computation and communication. Figure 8 illustrates a pipeline scheduling for distributed DP with 3 chunk-aggregation tasks following the processing stages in Table 2.

Performance Profiling. Pipeline-parallel aggregation enables the fine-grained scheduling of computation and com-

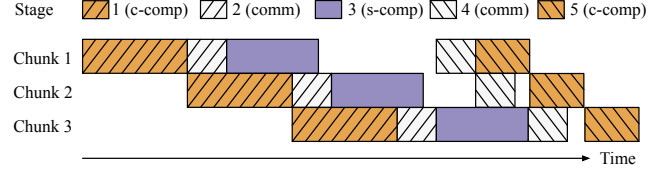


Figure 8: Pipeline scheduling of 3 chunk-aggregation tasks for distributed DP in 5 stages, as specified in Table 2.

munication. To achieve the maximum speedup, it is critical to determine the optimal number of chunks, m , used to partition a local update. To this end, Hyades first conducts the performance profiling and establishes the following performance model that empirically characterizes how the chunk processing time at a stage s , denoted by l_s , is related to m :

$$l_s = \beta_{s,1} \frac{d}{m} + \beta_{s,2} m + \beta_{s,3}, \quad (4)$$

where d is the update size (typically the same as the model size); $\beta_{s,1}, \beta_{s,2}$ and $\beta_{s,3}$ are the profiled parameters whose values depend on the hardware configurations and will be used to weigh the different terms described in the following. As indicated in Equation (4), our performance model breaks down the chunk processing time into three terms. The first term is in proportion to the chunk size d/m , which corresponds to the computation/communication overhead; the second term is in proportion to the number of chunks processed in parallel, which measures the delay caused by resource contention and interference; finally, the third term measures a constant processing overhead.

Determining the Optimal Number of Chunks. Using the performance model with parameters obtained via online profiling, Hyades can accurately predict the end-to-end aggregation time given the number of chunks. This helps Hyades search for the best number of chunks to configure. Specifically, denote a as the total number of stages in the aggregation workflow, $b_{s,c}$ and $f_{s,c}$ as the start and finish times of the stage $s \in [a]$ for chunk $c \in [m]$, respectively. To find the optimal number of chunks, m^* , Hyades solves the following optimization problem, which minimizes the end-to-end latency l that equates to the finish time of the last stage for the last chunk, i.e., $f_{a,m}$:

$$\begin{aligned} m^* &= \arg \min_{m \in \mathbb{N}_+} f_{a,m}, \\ \text{s.t. } f_{s,c} &= b_{s,c} + l_s \\ b_{s,c} &= \max\{o_{s,c}, r_{s,c}\}, \\ o_{s,c} &= \begin{cases} 0, & \text{if } s = 0, \\ f_{s-1,c}, & \text{otherwise,} \end{cases} \end{aligned} \quad (5)$$

$$r_{s,c} = \begin{cases} 0, & \text{if } s = 0 \text{ and } c = 0, \\ f_{q,m} \text{ or } \perp, & \text{if } s \neq 0 \text{ and } c = 0, \\ f_{s,c-1}, & \text{otherwise.} \end{cases} \quad (6)$$

Here, $q = \max_{i < s} \{i \mid r_i = r_s\}$ where r_s is the dominant resource of the stage s .³ Note that, constraint (5) is enforced as each chunk needs to sequentially go through the execution of all stages. Constraint (6) is enforced for achieving two other principles in the meantime: 1) each resource can be allocated to at most one chunk to execute a stage at any time, and 2) allocating the resource r to execute a stage s for a chunk c will be suspended, if there is another chunk c' which has not finished its execution of some previous stage $q < s$ that also uses the resource r . This optimization problem can be quickly solved by enumerating within a practical range (e.g., $m = 1, 2, \dots, 20$) provided that all l_s 's have been profiled.

5.3 DP-Compliant Clipping for Each Chunk

We intentionally design our distributed parallel architecture to perform only inter-coordinate operations (i.e., chunking, combining, and pipelining) on a model update, and thus it is orthogonal to most operations in the distributed DP which are coordinate-wise such as masking and noise addition. The only compatibility issue arises when it comes to *clipping* a chunked update, and we tackle this issue with a DP-compliant chunking scheme.

A Primer on Update Clipping. In the distributed DP for FL, the minimum required noise level is set by a function of the privacy parameters (e.g., ϵ and δ) in (ϵ, δ) -DP as well as the sensitivity of the aggregation (i.e., the maximum amount by which the aggregation can change due to the presence or absence of a client). As the sensitivity can hardly be decided a priori when training deep neural networks, each client needs to *clip* its update before uploading to the server for enforcing such a bound (i.e., sensitivity) [9]. For example, by clipping each client i 's raw update r_i to bound it within an L2-ball of radius c as follows:

$$\Delta_i = \begin{cases} \frac{c}{\|r_i\|_2} r_i, & \text{if } c < \|r_i\|_2, \\ r_i, & \text{otherwise,} \end{cases} \quad (7)$$

one can expect that the aggregate update $\Delta = \sum_i \Delta_i$ at the server also stays within an L2-ball of radius c despite changes in a client's participation. The minimum required noise level can be then determined based on this bound c .

Norm-Preserving Clipping. In our pipelined execution with the number of chunks set to m , a client's update is divided into m chunks, each of which is clipped separately. If one applies the original clipping bound c to each chunk of the update, the actual L2-norm of the entire update will be larger than c . This raises a privacy concern as the used noise level

which is computed based on the bound c becomes insufficient. To address this issue, we design a DP-compliant clipping scheme, which is chunking-aware and ensures the bound c for the entire update. Specifically, we set the clipping bound $c_{i,j}$ for each chunk $u_{i,j}$ of a local update u_i as: $c_{i,j} = \frac{\|u_{i,j}\|_2}{\|u_i\|_2} c$. This clipping scheme preserves the original clipping goal, i.e., the L2-norm of the entire update formed by combining all chunks is exactly c :

$$\sqrt{\sum_j c_{i,j}^2} = \sqrt{\frac{\sum_j \|u_{i,j}\|_2^2}{\|u_i\|_2^2} c^2} = c. \quad (8)$$

Altogether, this DP-compliant update clipping scheme makes our distributed parallel architecture compatible with the distributed DP in FL.

6 Implementation

Hyades is implemented in 9.3k lines of Python code. It leverages PyTorch [63] to instantiate FL applications and employs the distributed DP protocol with DSkellam [11], which integrates Skellam for noise mechanism and SecAgg for secure aggregation. This implementation is inline with the specifications outlined in [2, 8].

Efficiency is at the forefront of our system design, as we utilize multiprocessing and python-redis [7] for large model support, high pipeline parallelism, and the ability to accommodate a large number of clients. In Hyades, the server uses Socket.IO [6] for client communication and nginx [4] for load balancing I/O processes when handling client requests. The security primitives are built using two standard libraries Cryptography [1] and PyCryptodome [5]. Hyades has been open-sourced for community use via [3].

Programming Interface. Hyades offers a generic, user-friendly programming interface for developers to implement a variety of distributed DP protocols and privacy-sensitive applications that rely on differentially-private aggregate statistics. Specifically, developers can instantiate the abstract classes ProtocolServer and ProtocolClient by overwriting the event handlers to ensemble their distributed DP workflow. This design allows developers to concentrate on the computational logic while delegating the communications between the server and clients to the Hyades backend. Developers can also implement a new noise mechanism using different security primitives by overwriting the existing modules (e.g., DPHandler). Additionally, Hyades provides the flexibility to implement other privacy-sensitive applications beyond federated learning by simply extending the existing AppServer and AppClient classes and adding their own data processing logic. Further details can be found in Appendix D.

³We abort the second case in Constraint 6 if such q does not exist.

7 Evaluation

We evaluate Hyades’s effectiveness in various FL training tasks. The highlights of our evaluation are summarized below.

1. Our noise enforcement schemes ensure that the target privacy level is always achieved, even in the presence of client dropout, without compromising model utility (§7.2).
2. The pipeline-parallel aggregation design in Hyades significantly enhances the training speed, resulting in a $2.1 \times$ improvement in the average time of a training round (§7.3).
3. Hyades’s time-to-accuracy performance is comparable to that of its non-private counterpart (§7.4).

7.1 Methodology

Datasets and Models. We run two image classification applications of different sizes. The first dataset, CIFAR-10 [49], consists of 60k colored images categorized into 10 classes. We train a ResNet-18 [38] model with 11M parameters over 100 clients using a non-IID data distribution, generated by applying latent Dirichlet allocation (LDA) [10, 12, 39, 69] with concentration parameters set to 1.0 (i.e., label distributions highly skewed across clients). The second dataset, FEMNIST [20], consists of 805k greyscale images classified into 62 classes. The dataset was partitioned by the original data owners, and we merge every three owners’ data to form a client’s dataset. We train a CNN model [11, 45] with 1M parameters over 1000 clients.

Experiment Setup. We launch an AWS EC2 r5.4xlarge instance (16 vCPUs and 128 GB memory) for the server and one c5.xlarge (4 vCPUs and 8 GB memory) instance for each sampled client, aiming to match the computing power of mobile devices. To emulate hardware heterogeneity, we set the response latencies of clients to follow the Zipf distribution [41, 43, 53, 80] with $a = 1.2$ (moderately skewed). In this setting, the end-to-end latency of the i -th slowest client is proportional to i^{-a} . We also emulate network heterogeneity by throttling clients’ bandwidth to fall within the range [21Mbps, 210Mbps] to match the typical mobile bandwidth [27] and meanwhile follow another independent Zipf distribution with $a = 1.2$.

Hyperparameters. For FL training, we use the mini-batch SGD with momentum set to 0.9. The number of training rounds and local epochs are 50 and 2 for FEMNIST, and 150 and 1 for CIFAR-10, respectively. The batch size and learning rate are 20 and 0.01 for FEMNIST, and 128 and 0.005 for CIFAR-10, respectively.

For distributed DP, we set the privacy budget ϵ to 6 and δ the reciprocal of the total number of clients. We fix the signal bound multiplier $k = 3$, bias $\beta = e^{-0.5}$, and bit-width $b = 20$ for the configuration of DSkellam [11]. The L2-norm clipping bounds [11] for FEMNIST and CIFAR-10 are set to 1 and 3, respectively. Also, there are 100 and 16 clients being sampled in each round for FEMNIST and CIFAR-10, respectively.

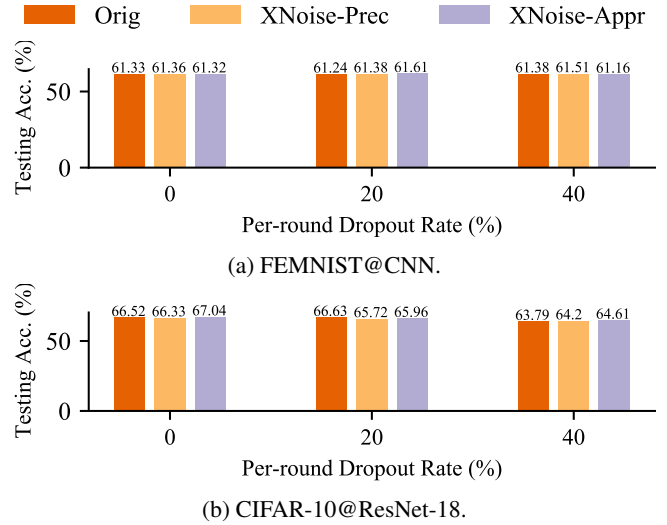


Figure 9: Final accuracy across various dropout outcomes.

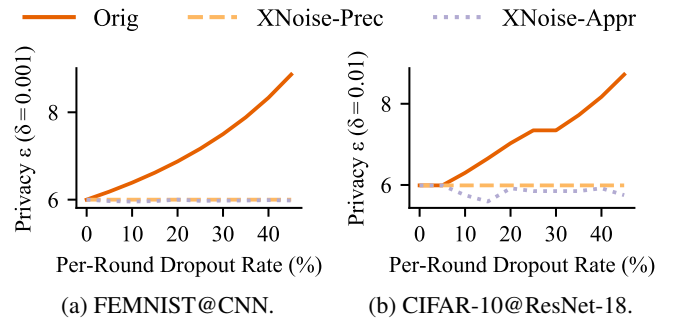


Figure 10: Privacy budget consumption. A larger ϵ corresponds to worse privacy preservation.

Baseline. We compare Hyades against Orig, the original, commonly-used distributed DP protocol that lacks the ability to enforce the target noise level (Definition 1 in §4) and support pipeline execution.

7.2 Effectiveness of Noise Enforcement

We first evaluate the effectiveness of Hyades’s dropout-resilient noise enforcement schemes (Xnoise-Prec and Xnoise-Appr). We vary the per-round dropout rate from 0 to 40% to simulate client dropout of various severities.

Xnoise-Prec Improves Privacy without Sacrificing Utility. Figure 10 depicts the end-to-end privacy budget consumption. As expected, XNoise-Prec precisely achieves the target privacy ($\epsilon = 6$) in all cases by effectively enforcing the target aggregate noise level (Theorem 1). On the other hand, due to the missing noise contributions from dropped clients, the overall privacy budget consumed by Orig explosively grows when client dropout becomes more severe. For example, when the dropout rate reaches 40%, training FEM-

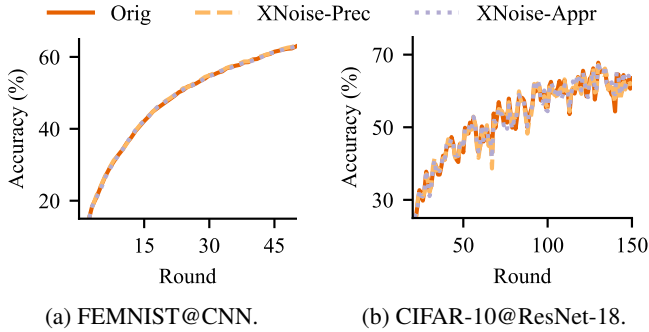


Figure 11: Round-to-accuracy performance (20% dropout).

NIST and CIFAR-10 to the preset number of rounds ends up consuming an ϵ of 8.3 and 8.2, respectively.

We also compare the final model accuracy across different protocols in Figure 9. Compared to Orig, which fails to achieve the target privacy in the presence of client dropout, our Xnoise-Prec converges at the same speed (as shown by the learning curves in Figure 11) and induces no more than 0.9% accuracy loss as it uses the minimum noise required to retain the target privacy. Also note that, in some cases, Xnoise-Prec achieves even higher accuracy than Orig despite the latter uses less noise. This is because the stochasticity introduced by excessive noise can work as a regularizer to reduce overfitting. In summary, XNoise-Prec addresses the aforementioned privacy issues of Orig in the presence of client dropout without compromising the final model utility.

Xnoise-Appr Achieves Comparable Improvements. Figure 10 shows that the privacy budget that Xnoise-Appr consumes is *no* more than the target value in all cases, because Xnoise-Appr never yields an insufficiently protected aggregate update (Theorem 2). Also, Xnoise-Appr induces a negligible loss in final model accuracy by at most 0.6% compared to Orig (Figure 9). This is because the noise used by Xnoise-Appr will not exceed the minimum necessary level by more than a factor of $O(1/n)$, where n is the number of sampled clients (Theorem 2). In summary, despite trading some precision in noise enforcement, XNoise-Appr achieves a comparable improvement of the privacy-utility tradeoff as that of Xnoise-Prec.

7.3 Efficiency of Pipeline Acceleration

We next evaluate the execution time of a training round in real deployments. To study the impact of model sizes, we additionally train a VGG-19 model [75] (20M parameters) over the CINIC-10 dataset [29]. The number of local epochs and batch size are set to 1 and 128, respectively.

Hyades Incurs Acceptable Overhead in Plain Execution without Pipelining. Figure 12 shows the average round time, broken down into two components: ‘agg’, related to

Table 3: End-to-end time-to-accuracy performance.

Dataset (Target Acc.)	Dropout Rate	Orig		XNoise-Prec		XNoise-Appr	
		plain	pipe	plain	pipe	plain	pipe
FEMNIST (62.8%)	0%	3.2h	3.0h	4.7h	4.4h	3.8h	3.6h
	20%	5.9h	5.7h	7.5h	7.4h	6.8h	6.8h
CIFAR-10 (68.3%)	0%	28.2h	19.3h	33.2h	20.8h	32.2h	20.7h
	20%	34.2h	23.3h	42.7h	27.0h	39.6h	25.1h

distributed DP operations, and ‘other’, related to remaining workflow operations such as model training. In a plain execution without pipeline acceleration, Xnoise-Prec extends the round time by less than 27% compared to Orig, if 20% clients drop after being sampled; the overhead becomes larger if no client drops, ranging from 16% to 49%. Despite this, we believe that the cost is still considered moderate and worth paying even *without* pipeline acceleration, as it ensures the target privacy is *always* enforced under unpredictable dropout dynamics.

Figure 12 also shows that XNoise-Appr reduces the runtime overhead of Xnoise-Prec by up to 25% by trading precision for reduced asymptotic complexity during noise enforcement (§4.3). Note that the speedup of Xnoise-Appr is not necessarily monotonic to the dropout severity as the number of noise components to be removed by Xnoise-Appr depends only on the binary representation of the number of dropped clients (Definition 3).

Hyades Significantly Benefits from Pipelining. Figure 12 shows that our pipeline acceleration benefits all the evaluated aggregation protocols in FL. With pipelining, Orig, XNoise-Prec, and Xnoise-Appr can be speeded up by up to 1.1 \times in FEMNIST, 1.6 \times in CIFAR-10, and 2.0 \times in CINIC-10, respectively, when no client drops out. Similarly, when 20% of clients drop out, the three protocols can be accelerated by up to 2.1 \times . These results lead to three key observations: 1) the execution of distributed DP can be significantly expedited by utilizing idle resources (§5.1); 2) larger models can enjoy more salient speedup due to increased improvement of resource utilization (e.g., a larger degree to which the uses of different resources can be overlapped); 3) both Xnoise-Prec and Xnoise-Appr have higher efficiency gains than Orig.

7.4 End-to-End Comparison

We finally compare the existing distributed DP solution (i.e., Orig with plain execution) against Hyades (XNoise-Prec or XNoise-Appr with pipeline acceleration) in an end-to-end comparison. We evaluate the time-to-accuracy performance, where the target FL accuracy is set to 62.8% in FEMNIST and 68.3% in CIFAR-10. These accuracy targets are set following the practice in [11] to meet our privacy target

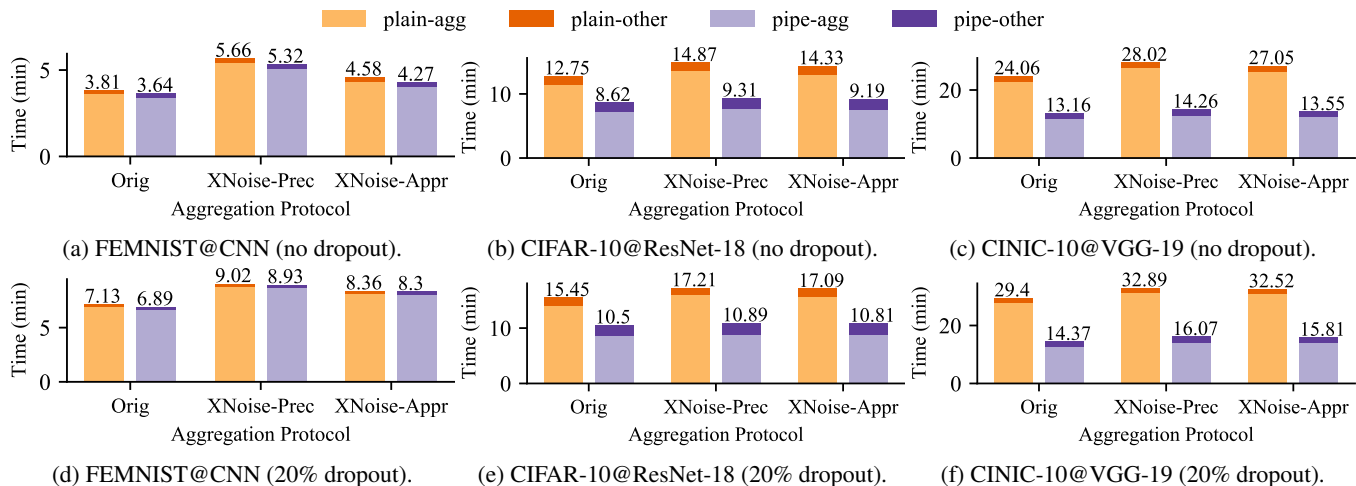


Figure 12: The breakdown of the training time of a round for **plain** execution and **pipeline** acceleration.

of 6. As this comparison would incur exceedingly high costs if performed in a large-scale real deployment with 100 or more clients over an extended period, we instead use the evaluation results in §7.2 and the runtime profiling results in §7.3 to project the total time needed to reach the target accuracy. Table 3 summarizes the results. Compared to the existing solution that is non-private under client dropout, Hyades using XNoise-Prec (resp. XNoise-Appr) consistently enforces the required privacy, while achieving the target accuracy with a moderate increase in training time of 25–38% (resp. 13–15%) in FEMNIST and even a reduction in training time of 21–26% (resp. 26–27%) in CIFAR-10. In conclusion, Hyades provides privacy protection with low or no cost to training efficiency.

8 Discussion and Future Work

Privacy Amplification via Subsampling. Privacy amplification via subsampling [82, 88] is commonly used to reduce the minimum required noise to be added in a central DP process. Specifically, it accounts for the uncertainty of a client’s identity resulting from client sampling to amplify its privacy against external adversaries. In distributed DP in FL, however, this technique does not directly apply as the server, who is responsible for client sampling and therefore has knowledge of each client’s identity, can also be an adversary. To address this issue, one solution is to use virtual client indexes that are refreshed after each round, making it challenging for the server to link the indexes to actual client identities. This can be achieved through the use of mix networks [23, 50], which may introduce new efficiency bottlenecks and we leave for future work.

Handling Mild Collusion. Hyades can be easily extended to address scenarios of mild collusion, where the server colludes with a small number of clients. In real-world deploy-

ments, the number of clients is usually large, and the chance of having a colluded client sampled by the server is small⁴ (e.g., tens to hundreds of clients sampled from millions of devices [18, 47]). Given that only a small fraction of participants (e.g., <1%) can potentially collude, clients can slightly increase the noise added to their updates to compensate the potential privacy loss due to collusion, without compromising the model utility.

Protecting against Dishonest Adversary. To address the potential threat posed by a dishonest adversary that deviates from the protocol, Hyades needs to ensure that: 1) each sampled client adds an adequate amount of local noise, and 2) the server correctly informs each surviving client of the dropout outcome. Zero-knowledge proofs [35] can be used to achieve these objectives, which we leave for future work.

9 Related Work

Differentially Private FL. The topic of differentially private FL (DPFL) has seen a surge of interest in recent years. DP-FedAvg [57, 68] is the first system to use central DP for protecting FL. Assuming the same threat model, Distributed DP-SGD [15] and DP-FTRL [46] address the technical challenges brought by uniform client sampling and provide alternative methods for privacy amplification. Unlike these works, Hyades does not assume a trusted server.

Many studies in the topic of distributed DP for private FL focus on secure aggregation and DP algorithm design. To name a few, DDGauss [45] and DSkellam [11] provide end-to-end privacy analysis by combining the DP noise addition with SecAgg. FLDP [79] explores aggregation based on the

⁴An honest-but-curious server does not intentionally sample colluded clients since it needs to follow the sampling algorithm faithfully.

learning with errors (LWE) problem [70], using residual errors as DP noise. Hyades complements these works by providing dropout resilience and improved execution efficiency.

The work closest to Hyades is [14] which tackles the dropout resilience problem in distributed DP also using an ‘add-then-remove’ noise enforcement approach. Unlike Hyades, as discussed in §4.1, this approach adopts a ‘strawman’ design that is incompatible with transmitting noise seeds (thus, poor efficiency) and does not assume client dropout during noise removal (thus, poor robustness). Hyades addresses these problems using the ‘noise decomposition’ design for noise enforcement, while optimizing the system efficiency of distributed DP.

Data Analytics with Distributed DP. Beyond FL, systems such as Honeycrisp [71] and Orchard [72] also compute privacy-preserving statistics from distributed data without trusted parties. However, these systems use additively homomorphic encryption for secure aggregation, which does not scale well with high-dimensional data. In contrast, Hyades provides a lightweight solution for high-dimensional data that offers improved execution efficiency.

10 Conclusion

Distributed differential privacy has long been appealing to federated learning as it achieves an informed privacy-utility tradeoff without a trusted server. This paper presents Hyades, an efficient FL framework that enables dropout-resilient distributed DP in realistic FL scenarios. To handle client dropout, Hyades designs a novel and efficient “add-then-remove” approach to enforce the required noise at the target level precisely, or approximately with a tight bound, regardless of client dropout. Hyades also enables pipeline parallelism for accelerated secure aggregation with an efficient distributed parallel architecture. Compared to the existing distributed DP mechanisms in FL, Hyades efficiently achieves the highest training accuracy without compromising privacy guarantees in the presence of client dropout.

References

- [1] Cryptography. <https://cryptography.io/>.
- [2] Google research. <https://github.com/google-research/google-research>.
- [3] Hyades codebase. <https://github.com/SamuelGong/Hyades>.
- [4] Nginx: Advanced load balancer, web server, and reverse proxy. <https://www.nginx.com/>.
- [5] Pycryptodome. <https://www.pycryptodome.org/>.
- [6] Python socket.io server and client. <https://github.com/miguelgrinberg/python-socketio>.
- [7] Redis in-memory data structure store. <https://redis.io/>.
- [8] Tensorflow privacy. <https://github.com/tensorflow/privacy>.
- [9] Martin Abadi, Andy Chu, Ian Goodfellow, H Brendan McMahan, Ilya Mironov, Kunal Talwar, and Li Zhang. Deep learning with differential privacy. In *CCS*, 2016.
- [10] Durmus Alp Emre Acar, Yue Zhao, Ramon Matas Navarro, Matthew Mattina, Paul N Whatmough, and Venkatesh Saligrama. Federated learning based on dynamic regularization. In *ICLR*, 2021.
- [11] Naman Agarwal, Peter Kairouz, and Ziyu Liu. The Skellam mechanism for differentially private federated learning. In *NeurIPS*, 2021.
- [12] Maruan Al-Shedivat, Jennifer Gillenwater, Eric Xing, and Afshin Rostamizadeh. Federated learning via posterior averaging: A new perspective and practical algorithms. In *ICLR*, 2020.
- [13] Arm. Trustzone technology. <https://developer.arm.com/ip-products/security-ip/trustzone>, 2021.
- [14] Chunghun Baek, Sungwook Kim, Dongkyun Nam, and Jihoon Park. Enhancing differential privacy for federated learning at scale. *IEEE Access*, 2021.
- [15] Borja Balle, Peter Kairouz, Brendan McMahan, Om Thakkar, and Abhradeep Guha Thakurta. Privacy amplification via random check-ins. In *NeurIPS*, 2020.
- [16] James Henry Bell, Kallista A Bonawitz, Adrià Gascón, Tancrede Lepoint, and Mariana Raykova. Secure single-server aggregation with (poly) logarithmic overhead. In *CCS*, 2020.

- [17] Andrea Bittau, Úlfar Erlingsson, Petros Maniatis, Ilya Mironov, Ananth Raghunathan, David Lie, Mitch Rudominer, Ushasree Kode, Julien Tinnes, and Bernhard Seefeld. Prochlo: Strong privacy for analytics in the crowd. In *SOSP*, 2017.
- [18] Keith Bonawitz, Hubert Eichner, Wolfgang Grieskamp, Dzmitry Huba, Alex Ingerman, Vladimir Ivanov, Chloe Kiddon, Jakub Konečný, Stefano Mazzocchi, Brendan McMahan, et al. Towards federated learning at scale: System design. In *MLSys*, 2019.
- [19] Keith Bonawitz, Vladimir Ivanov, Ben Kreuter, Antonio Marcedone, H Brendan McMahan, Sarvar Patel, Daniel Ramage, Aaron Segal, and Karn Seth. Practical secure aggregation for privacy-preserving machine learning. In *CCS*, 2017.
- [20] Sebastian Caldas, Sai Meher Karthik Duddu, Peter Wu, Tian Li, Jakub Konečný, H Brendan McMahan, Virginia Smith, and Ameet Talwalkar. Leaf: A benchmark for federated settings. In *NeurIPS Workshop*, 2019.
- [21] Nicholas Carlini, Chang Liu, Úlfar Erlingsson, Jernej Kos, and Dawn Song. The secret sharer: Evaluating and testing unintended memorization in neural networks. In *USENIX Security*, 2019.
- [22] Zheng Chai, Ahsan Ali, Syed Zawad, Stacey Truex, Ali Anwar, Nathalie Baracaldo, Yi Zhou, Heiko Ludwig, Feng Yan, and Yue Cheng. Tifl: A tier-based federated learning system. In *HPDC*, 2020.
- [23] David L Chaum. Untraceable electronic mail, return addresses, and digital pseudonyms. *Communications of the ACM*, 24(2):84–90, 1981.
- [24] Zitai Chen, Georgios Vasilakis, Kit Murdock, Edward Dean, David Oswald, and Flavio D Garcia. Voltpillager: Hardware-based fault injection attacks against intel sgx enclaves using the svid voltage scaling interface. In *USENIX Security*, 2021.
- [25] Albert Cheu, Adam Smith, Jonathan Ullman, David Zerber, and Maxim Zhilyaev. Distributed differential privacy via shuffling. In *Eurocrypt*, 2019.
- [26] Beongjun Choi, Jy-yong Sohn, Dong-Jun Han, and Jaekyun Moon. Communication-computation efficient secure aggregation for federated learning. *arXiv:2012.05433*, 2020.
- [27] Cisco. Cisco annual internet report (2018–2023) white paper, 2020. <https://support.google.com/messages/answer/9327902>.
- [28] Cynthia Dwork. Differential privacy. *Automata, languages and programming*, pages 1–12, 2006.
- [29] Luke N Darlow, Elliot J Crowley, Antreas Antoniou, and Amos J Storkey. Cinic-10 is not imagenet or cifar-10. *arXiv:1810.03505*, 2018.
- [30] Jieren Deng, Yijue Wang, Ji Li, Chenghong Wang, Chao Shang, Hang Liu, Sanguthevar Rajasekaran, and Caiwen Ding. Tag: Gradient attack on transformer-based language models. In *EMNLP*, 2021.
- [31] Dimitar I Dimitrov, Mislav Balunović, Nikola Jovanović, and Martin Vechev. Lamp: Extracting text from gradients with language model priors. *arXiv:2202.08827*, 2022.
- [32] Cynthia Dwork, Frank McSherry, Kobbi Nissim, and Adam Smith. Calibrating noise to sensitivity in private data analysis. In *Theory of cryptography conference*, pages 265–284. Springer, 2006.
- [33] Cynthia Dwork and Aaron Roth. The algorithmic foundations of differential privacy. *Foundations and Trends in Theoretical Computer Science*, 9(3–4):211–407, 2014.
- [34] Úlfar Erlingsson, Vitaly Feldman, Ilya Mironov, Ananth Raghunathan, Kunal Talwar, and Abhradeep Thakurta. Amplification by shuffling: From local to central differential privacy via anonymity. In *SODA*, 2019.
- [35] Shafi Goldwasser, Silvio Micali, and Chales Rackoff. The knowledge complexity of interactive proof-systems. In *Providing Sound Foundations for Cryptography: On the Work of Shafi Goldwasser and Silvio Micali*, pages 203–225. 2019.
- [36] Google. Your chats stay private while messages improves suggestions, 2021. <https://support.google.com/messages/answer/9327902>.
- [37] Samyak Gupta, Yangsibo Huang, Zexuan Zhong, Tianyu Gao, Kai Li, and Danqi Chen. Recovering private text in federated learning of language models. *arXiv:2205.08514*, 2022.
- [38] Kaiming He, Xiangyu Zhang, Shaoqing Ren, and Jian Sun. Deep residual learning for image recognition. In *CVPR*, 2016.
- [39] Tzu-Ming Harry Hsu, Hang Qi, and Matthew Brown. Measuring the effects of non-identical data distribution for federated visual classification. *arXiv:1909.06335*, 2019.
- [40] Intel. Software guard extensions. <https://software.intel.com/content/www/us/en/develop/topics/software-guard-extensions.html>, 2021.
- [41] Zhipeng Jia and Emmett Witchel. Boki: Stateful serverless computing with shared logs. In *SOSP*, 2021.

- [42] Zhifeng Jiang, Wei Wang, Baochun Li, and Bo Li. Pisces: Efficient federated learning via guided asynchronous training. In *SoCC*, 2022.
- [43] Zhifeng Jiang, Wei Wang, Bo Li, and Qiang Yang. Towards efficient synchronous federated training: A survey on system optimization strategies. *IEEE Transactions on Big Data*, 2022.
- [44] Swanand Kadhe, Nived Rajaraman, O Ozan Koyluoglu, and Kannan Ramchandran. Fastsecagg: Scalable secure aggregation for privacy-preserving federated learning. *arXiv:2009.11248*, 2020.
- [45] Peter Kairouz, Ziyu Liu, and Thomas Steinke. The distributed discrete gaussian mechanism for federated learning with secure aggregation. In *ICML*, 2021.
- [46] Peter Kairouz, Brendan McMahan, Shuang Song, Om Thakkar, Abhradeep Thakurta, and Zheng Xu. Practical and private (deep) learning without sampling or shuffling. In *ICML*, 2021.
- [47] Peter Kairouz, H Brendan McMahan, Brendan Avent, Aurélien Bellet, Mehdi Bennis, Arjun Nitin Bhagoji, Keith Bonawitz, Zachary Charles, Graham Cormode, Rachel Cummings, et al. Advances and open problems in federated learning. *Foundations and Trends in Machine Learning*, 14(1), 2021.
- [48] Young Geun Kim and Carole-Jean Wu. Autoff: Enabling heterogeneity-aware energy efficient federated learning. In *MICRO*, 2021.
- [49] Alex Krizhevsky, Geoffrey Hinton, et al. Learning multiple layers of features from tiny images. 2009.
- [50] Albert Kwon, David Lazar, Srinivas Devadas, and Bryan Ford. Riffle. In *PETS*, 2016.
- [51] Fan Lai, Yinwei Dai, Sanjay S Singapuram, Jiachen Liu, Xiangfeng Zhu, Harsha V Madhyastha, and Mosharaf Chowdhury. FedScale: Benchmarking model and system performance of federated learning at scale. In *ICML*, 2022.
- [52] Fan Lai, Xiangfeng Zhu, Harsha V. Madhyastha, and Mosharaf Chowdhury. Oort: Efficient federated learning via guided participant selection. In *OSDI*, 2021.
- [53] Yunseong Lee, Alberto Scolari, Byung-Gon Chun, Marco Domenico Santambrogio, Markus Weimer, and Matteo Interlandi. Pretzel: Opening the black box of machine learning prediction serving systems. In *OSDI*, 2018.
- [54] Wenqi Li, Fausto Milletari, Daguang Xu, Nicola Rieke, Jonny Hancox, Wentao Zhu, Maximilian Baust, Yan Cheng, Sébastien Ourselin, M Jorge Cardoso, et al. Privacy-preserving federated brain tumour segmentation. In *MLMI Workshop*, 2019.
- [55] Heiko Ludwig, Nathalie Baracaldo, Gegi Thomas, Yi Zhou, Ali Anwar, Shashank Rajamoni, Yuya Ong, Jayaram Radhakrishnan, Ashish Verma, Mathieu Sinn, et al. Ibm federated learning: an enterprise framework white paper v0.1. *arXiv:2007.10987*, 2020.
- [56] Brendan McMahan, Eider Moore, Daniel Ramage, Seth Hampson, and Blaise Aguera y Arcas. Communication-efficient learning of deep networks from decentralized data. In *AISTATS*, 2017.
- [57] H Brendan McMahan, Daniel Ramage, Kunal Talwar, and Li Zhang. Learning differentially private recurrent language models. In *ICLR*, 2018.
- [58] Luca Melis, Congzheng Song, Emiliano De Cristofaro, and Vitaly Shmatikov. Exploiting unintended feature leakage in collaborative learning. In *IEEE S&P*, 2019.
- [59] Ralph C Merkle. Secure communications over insecure channels. *Communications of the ACM*, 21(4):294–299, 1978.
- [60] Ilya Mironov. Rényi differential privacy. In *2017 IEEE 30th computer security foundations symposium (CSF)*, pages 263–275. IEEE, 2017.
- [61] Milad Nasr, Reza Shokri, and Amir Houmansadr. Comprehensive privacy analysis of deep learning: Passive and active white-box inference attacks against centralized and federated learning. In *IEEE S&P*, 2019.
- [62] NVIDIA. Triaging covid-19 patients: 20 hospitals in 20 days build ai model that predicts oxygen needs, 2020. <https://blogs.nvidia.com/blog/2020/10/05/federated-learning-covid-oxygen-needs/>.
- [63] Adam Paszke, Sam Gross, Francisco Massa, Adam Lerer, James Bradbury, Gregory Chanan, Trevor Killeen, Zeming Lin, Natalia Gimelshein, Luca Antiga, et al. Pytorch: An imperative style, high-performance deep learning library. In *NeurIPS*, 2019.
- [64] Matthias Paulik, Matt Seigel, Henry Mason, Dominic Telaar, Joris Kluivers, Rogier van Dalen, Chi Wai Lau, Luke Carlson, Filip Granqvist, Chris Vandeveld, et al. Federated evaluation and tuning for on-device personalization: System design & applications. *arXiv:2102.08503*, 2021.
- [65] Le Trieu Phong, Yoshinori Aono, Takuya Hayashi, Lihua Wang, and Shiho Moriai. Privacy-preserving deep learning via additively homomorphic encryption. *IEEE Transactions on Information Forensics and Security*, 13(5):1333–1345, 2018.

- [66] Vasyi Pihur, Aleksandra Korolova, Frederick Liu, Subhash Sankuratripati, Moti Yung, Dachuan Huang, and Ruogu Zeng. "Differentially-private" draw and discard" machine learning. *arXiv:1807.04369*, 2018.
- [67] Aurick Qiao, Bryon Aragam, Bingjing Zhang, and Eric Xing. Fault tolerance in iterative-convergent machine learning. In *ICML*, 2019.
- [68] Swaroop Ramaswamy, Om Thakkar, Rajiv Mathews, Galen Andrew, H Brendan McMahan, and Franoise Beaufays. Training production language models without memorizing user data. *arXiv:2009.10031*, 2020.
- [69] Sashank J Reddi, Zachary Charles, Manzil Zaheer, Zachary Garrett, Keith Rush, Jakub Koneny, Sanjiv Kumar, and Hugh Brendan McMahan. Adaptive federated optimization. In *ICLR*, 2020.
- [70] Oded Regev. On lattices, learning with errors, random linear codes, and cryptography. *Journal of the ACM*, 56(6):1–40, 2009.
- [71] Edo Roth, Daniel Noble, Brett Hemenway Falk, and Andreas Haeberlen. Honeycrisp: large-scale differentially private aggregation without a trusted core. In *SOSP*, 2019.
- [72] Edo Roth, Hengchu Zhang, Andreas Haeberlen, and Benjamin C Pierce. Orchard: Differentially private analytics at scale. In *OSDI*, 2020.
- [73] Adi Shamir. How to share a secret. *Communications of the ACM*, 22(11):612–613, 1979.
- [74] Reza Shokri, Marco Stronati, Congzheng Song, and Vitaly Shmatikov. Membership inference attacks against machine learning models. In *IEEE S&P*, 2017.
- [75] Karen Simonyan and Andrew Zisserman. Very deep convolutional networks for large-scale image recognition. *arXiv:1409.1556*, 2014.
- [76] Jinhyun So, Baak Gler, and A Salman Avestimehr. Turbo-aggregate: Breaking the quadratic aggregation barrier in secure federated learning. *IEEE Journal on Selected Areas in Information Theory*, 2(1):479–489, 2021.
- [77] Jinhyun So, Corey J Nolet, Chien-Sheng Yang, Songze Li, Qian Yu, Ramy E Ali, Basak Guler, and Salman Avestimehr. Lightsecagg: a lightweight and versatile design for secure aggregation in federated learning. In *MLSys*, 2022.
- [78] Congzheng Song and Vitaly Shmatikov. Auditing data provenance in text-generation models. In *SIGKDD*, 2019.
- [79] Timothy Stevens, Christian Skalka, Christelle Vincent, John Ring, Samuel Clark, and Joseph Near. Efficient differentially private secure aggregation for federated learning via hardness of learning with errors. In *USENIX Security*, 2022.
- [80] Huangshi Tian, Minchen Yu, and Wei Wang. Crystalperf: Learning to characterize the performance of dataflow computation through code analysis. In *ATC*, 2021.
- [81] Jo Van Bulck, Marina Minkin, Ofir Weisse, Daniel Genkin, Baris Kasikci, Frank Piessens, Mark Silberstein, Thomas F Wenisch, Yuval Yarom, and Raoul Strackx. Foreshadow: Extracting the keys to the intel sgx kingdom with transient out-of-order execution. In *USENIX Security*, 2018.
- [82] Yu-Xiang Wang, Borja Balle, and Shiva Prasad Kasiviswanathan. Subsampled Rnyi differential privacy and analytical moments accountant. In *AISTATS*, 2019.
- [83] Zhibo Wang, Mengkai Song, Zhifei Zhang, Yang Song, Qian Wang, and Hairong Qi. Beyond inferring class representatives: User-level privacy leakage from federated learning. In *INFOCOM*, 2019.
- [84] WeBank. Utilization of fate in anti money laundering through multiple banks, 2020. <https://www.fedai.org/cases/utilization-of-fate-in-anti-money-laundering-through-multiple-banks/>.
- [85] Chengxu Yang, Qipeng Wang, Mengwei Xu, Zhenpeng Chen, Kaigui Bian, Yunxin Liu, and Xuanzhe Liu. Characterizing impacts of heterogeneity in federated learning upon large-scale smartphone data. In *WWW*, 2021.
- [86] Jiayuan Ye, Aadyaa Maddi, Sasi Kumar Murakonda, and Reza Shokri. Enhanced membership inference attacks against machine learning models. In *CCS*, 2022.
- [87] Ligeng Zhu, Zhijian Liu, and Song Han. Deep leakage from gradients. In *NeurIPS*, 2019.
- [88] Yuqing Zhu and Yu-Xiang Wang. Poission subsampled Rnyi differential privacy. In *ICML*, 2019.

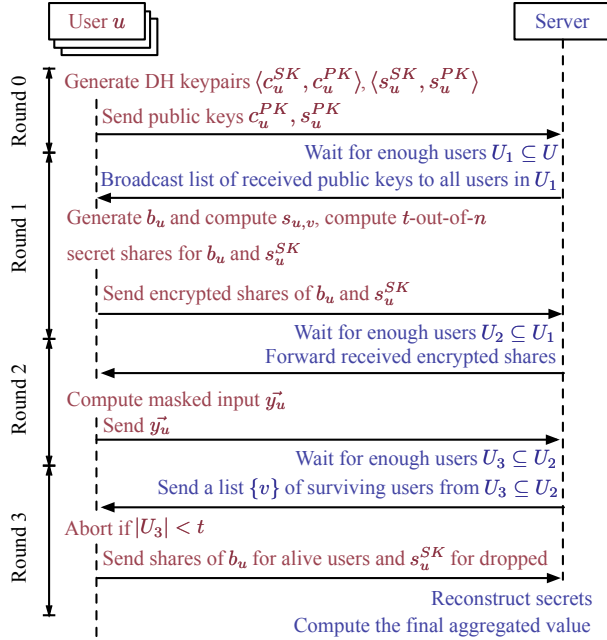


Figure 13: SecAgg’s protocol in the semi-honest threat model [19].

A The SecAgg protocol

Technical Details. Here we provide a detailed description of how SecAgg [19] works under the semi-honest adversary. As depicted in Fig. 13, the protocol consists of four communication rounds.

- *Round 0 (Advertise Keys):* each client $u \in U$ generates key pairs $\langle c_u^{SK}, c_u^{PK} \rangle, \langle s_u^{SK}, s_u^{PK} \rangle$ and sends (c_u^{PK}, s_u^{PK}) to all of her neighbors with the relaying help of the server.
- *Round 1 (Share Keys):* each of the alive clients $u \in U_1 \subseteq U$ runs the Diffie-Hellman key agreement protocol [59] that derives a shared random key $s_{u,v} = \mathcal{KA}.\text{Agree}(s_u^{SK}, s_v^{PK})$ for every other client $v \in U_1$.⁵ Client u also randomly samples a seed b_u , and securely shares s_u^{SK} and b_u to each of the other client v ’s by sending it the respective t -out-of- n shares encrypted using the corresponding agreed key $\mathcal{KA}.\text{Agree}(c_u^{SK}, c_v^{PK})$ ’s.
- *Round 2 (Masked Input Collection):* each surviving client $u \in U_2$ prepares a pairwise mask $\vec{m}_{u,v} = \text{PRG}(s_{u,v})$ derived from shared keys with each of the other client v ’s. She also generates a self mask $\vec{r}_u = \text{PRG}(b_u)$, masks her vector input \vec{x}_u in the following manner and then sends the masked input \vec{y}_u to the server:

$$\vec{y}_u = \vec{x}_u + \vec{r}_u - \sum_{v < u, v \in U_2} \vec{m}_{u,v} + \sum_{v > u, v \in U_2} \vec{m}_{u,v}. \quad (9)$$

⁵Note that $\mathcal{KA}.\text{Agree}(\cdot, \cdot)$ is symmetric and thus $s_{u,v} = s_{v,u}$

- *Round 3 (Unmasking):* summing up masked inputs submitted by surviving clients U_3 , the server obtains:

$$\sum_{u \in U_3} \vec{x}_u + \underbrace{\sum_{u \in U_3} \vec{r}_u}_A + \underbrace{\sum_{u \in U_2/U_3} \left(\sum_{v < u, v \in U_3} \vec{m}_{u,v} - \sum_{v > u, v \in U_3} \vec{m}_{u,v} \right)}_B. \quad (10)$$

Then, to remove part A, for each surviving client $u \in U_3$, the server compute \vec{r}_u by reconstructing b_u with over t shares of it collected from surviving clients U_4 . Similarly, to remove part B, for each dropped clients $u \in U_2/U_3$, the server reconstructs its secret key c_u^{SK} by collecting over t shares of it from U_4 . Together with the public keys of v ’s from $U_2/\{u\}$ to reconstruct $s_{u,v}$ ’s, the server finally computes and removes all the related $\vec{m}_{u,v}$ ’s.

Source of Complexity. We now pinpoint two main sources of SecAgg’s inefficiency (§2.3). The first source is the use of Shamir’s t -out-of- n secret sharing scheme [73] (Round 1). It is employed to gain resilience against client dropout, as it allows a secret to be split and shared to n clients so that any t clients can provide enough information to reconstruct it. For a client, generating Shamir’s t -out-of- n secret takes $O(n^2)$ time, yielding a quadratic computation overhead w.r.t. the number of sampled clients ($O(|U_1|^2)$). The second source is the design of *pairwise masking*, where each client adds a pairwise mask (of the same length d as the model) to her update for each of the other alive clients (Round 2), and the server needs to unmask these masks for each dropped client (Round 3). This helps tolerate colluding parties, as the pairwise masks between any two benign clients will be concealed from the adversary. However, it induces quadratic computation overhead to both clients ($O(d|U_2|^2)$) and the server ($O(d|U_3|^2)$).

B Noise Enforcement Complexity Analysis

We first evaluate the complexity of XNoise-Prec (§4.2). All calculations below assume a single server and $|S|$ users, where $|D| = O(|S|)$ clients drop out after being sampled. We also use d to denote the number of parameters in a model. We ignore the cost of the used public key infrastructure but stress that including its cost does not change any of the asymptotics.

For a sampled client, its computational cost stems from (1) generating noise components, which is $O(|S|)$, (2) adding the noise components to its update, which is $O(d|S|)$ where d is the model size, measured by the number of model parameters, and (3) creating secret shares for the used PRG seeds, which is $O(|S|^3)$. Together, the computational complexity is $O(d|S| + |S|^3)$. Concerning the communication cost, it stems from (1) uploading the needed seeds for noise removal, which is $O(|S|)$, and, if necessary, (2) uploading the secret shares for recovering the other clients’ missing seeds, which is $O(|S|^2)$. The overall communication complexity is hence $O(|S|^2)$.

For the server, its computational cost stems from (1) recovering the missing seeds, if any, using the optimized reconstruction technique given in [19], which is $O(|S|^3)$, and (2) generating excessive noise components using the PRG seeds and removing them, which is $O(d|S|^2)$. Thus, the overall computational complexity is $O(|S|^3 + d|S|^2)$. As for the server's communication cost, it stems from (1) receiving PRG seeds from surviving clients, which is $O(|S|^2)$, and (2) receiving secret shares for recovering the missing seeds (if any), which is $O(|S|^3)$. Overall, the communication complexity is $O(|S|^3)$.

The analysis of XNoise-Appr (§4.3) is almost the same as the above, except that each client generates $O(\log|S|)$ noise components instead of $O(|S|)$. We thus omit it for brevity.

C Proofs for Noise Enforcement Results

Proof for Theorem 1 (§4.2).

Proof. Before the server performs noise deduction, the aggregated update is randomized with noise level:

$$\begin{aligned} & \sum_{c_j \in S \setminus D} \left(\frac{\sigma_*^2}{|S|} + \sum_{k=1}^t \frac{\sigma_*^2}{(|S|-k+1)(|S|-k)} \right) \\ &= \sum_{c_j \in S \setminus D} \left(\frac{\sigma_*^2}{|S|} + \sum_{k=1}^t \left(\frac{\sigma_*^2}{|S|-k} - \frac{\sigma_*^2}{|S|-k+1} \right) \right) \\ &= \sigma_*^2 (|S| - |D|) \left(\frac{1}{|S|} + \frac{1}{|S|-t} - \frac{1}{|S|} \right) = \sigma_*^2 \frac{|S|-|D|}{|S|-t}. \end{aligned}$$

Moreover, the total noise level deducted by the server is:

$$\begin{aligned} & \sum_{c_j \in S \setminus D} \sum_{k=|D|+1}^t \frac{\sigma_*^2}{(|S|-k+1)(|S|-k)} \\ &= (|S|-|D|) \sigma_*^2 \sum_{k=|D|+1}^t \left(\frac{1}{|S|-k} - \frac{1}{|S|-k+1} \right). \\ &= (|S|-|D|) \sigma_*^2 \left(\frac{1}{|S|-t} - \frac{1}{|S|-|D|} \right) = \sigma_*^2 \frac{t-|D|}{|S|-t}. \end{aligned}$$

Thus, the remaining noise level at the aggregated update is $\sigma_*^2 \frac{|S|-|D|}{|S|-t} - \sigma_*^2 \frac{t-|D|}{|S|-t} = \sigma_*^2$. \square

Proof for Theorem 2 (§4.3).

Proof. Before the server performs noise deduction, the aggregated update is randomized with noise level:

$$\begin{aligned} & \sum_{c_j \in S \setminus D} \left(\frac{\sigma_*^2}{|S|} + \eta + \sum_{k=2}^{\tau+1} \eta \cdot 2^{k-2} \right) \\ &= \sum_{c_j \in S \setminus D} \left(\frac{\sigma_*^2}{|S|} + 2^\tau \eta \right) \\ &= (|S|-|D|) \left(\frac{\sigma_*^2}{|S|} + 2^\tau \frac{\sigma_*^2 t}{2^\tau |S| (|S|-t)} \right) = \sigma_*^2 \frac{|S|-|D|}{|S|-t}. \end{aligned}$$

As for noise deduction by the server, we discuss two cases.

Case 1: First, if there is no client dropping ($|D|=0$), the total noise level that can be deducted is:

$$\begin{aligned} & \sum_{c_j \in S} \left(\eta + \sum_{k=2}^{\tau+1} 2^{k-2} \eta \right) \\ &= \sum_{c_j \in S} 2^\tau \eta = |S| 2^\tau \frac{\sigma_*^2 t}{2^\tau |S| (|S|-t)} = \sigma_*^2 \frac{t}{|S|-t}. \end{aligned}$$

Thus, after the noise deduction, the remaining noise level at the aggregated update is exactly:

$$\sigma_*^2 \frac{|S|}{|S|-t} - \sigma_*^2 \frac{t}{|S|-t} = \sigma_*^2.$$

Case 2: Next, we consider the case where $|D| > 0$ clients drop. In this case, the total noise level that can be deducted is:

$$\sum_{c_j \in S \setminus D} \sum_{k=2}^{\tau+1} 2^{k-2} \eta \mathbb{1}(b_{k-1}=1) = \sum_{c_j \in S \setminus D} \left[\frac{\lambda}{\eta} \right] \eta.$$

Denoting this quantity by m . On the one hand, we have:

$$\begin{aligned} m &= \sum_{c_j \in S \setminus D} \left[\frac{\lambda}{\eta} \right] \eta \leq \sum_{c_j \in S \setminus D} [\lambda] \leq \sum_{c_j \in S \setminus D} \lambda \\ &= (|S|-|D|) \frac{(t-|D|) \sigma_*^2}{(|S|-t)(|S|-|D|)} = \sigma_*^2 \frac{t-|D|}{|S|-t}. \end{aligned}$$

Thus, the remaining noise level has a lower bound:

$$\sigma_*^2 \frac{|S|-|D|}{|S|-t} - m \geq \sigma_*^2 \frac{|S|-|D|}{|S|-t} - \sigma_*^2 \frac{t-|D|}{|S|-t} = \sigma_*^2.$$

On the other hand, we also have:

$$\begin{aligned} m &= \sum_{c_j \in S \setminus D} \left[\frac{\lambda}{\eta} \right] \eta > \sum_{c_j \in S \setminus D} \left(\frac{\lambda}{\eta} - 1 \right) \eta = \sum_{c_j \in S \setminus D} (\lambda - \eta) \\ &= (|S|-|D|) \left(\frac{(t-|D|) \sigma_*^2}{(|S|-t)(|S|-|D|)} - \frac{\sigma_*^2 t}{2^\tau |S| (|S|-t)} \right) \\ &= (|S|-|D|) \frac{\sigma_*^2}{|S|-t} \left(\frac{t-|D|}{|S|-|D|} - \frac{t}{2^\tau |S|} \right) \\ &\geq (|S|-|D|) \frac{\sigma_*^2}{|S|-t} \left(\frac{t-|D|}{|S|-|D|} - \frac{1}{|S|} \right) \\ &= \frac{\sigma_*^2}{|S|-t} \left(t-|D| - \frac{|S|-|D|}{|S|} \right) \geq \frac{\sigma_*^2}{|S|-t} (t-|D|-1). \end{aligned}$$

Thus, after noise deduction, the remaining noise level also has an upper bound:

$$\begin{aligned} & \sigma_*^2 \frac{|S|-|D|}{|S|-t} - m \\ &< \sigma_*^2 \frac{|S|-|D|}{|S|-t} - \frac{\sigma_*^2}{|S|-t} (t-|D|-1) \\ &= \sigma_*^2 \frac{|S|-|D|}{|S|-t} - \sigma_*^2 \frac{t-|D|}{|S|-t} + \frac{\sigma_*^2}{|S|-t} = \sigma_*^2 + \frac{\sigma_*^2}{|S|-t}. \end{aligned}$$

\square

D Generic Programming Interface

Support for Diverse Distributed DP Algorithms. As mentioned in Section 6, developers can implement customized

Table 4: The programming interface provided for developers to customize their own distributed DP algorithms and applications.

Category	Base Class	Customization Instruction
Distributed DP	ProtocolServer	Overwrite <code>set_graph_dict()</code> to specify the distributed DP workflow for pipeline plan generation. Create one method for coordinating each operation, e.g., <code>encode_data()</code> to instruct DP encoding.
	ProtocolClient	Overwrite <code>set_routine()</code> to specify the handler for each server’s request. Create one method for processing each server’s request, e.g., <code>encode_data()</code> to encode local input on request.
	DPHandler	Overwrite <code>init_params()</code> to specify how to initialize DP parameters, <code>encode_data()</code> and <code>decode_data()</code> to how to perform DP encoding and decoding given a chunk of input, respectively.
	AEHandler, KAHandler, PGHandler, SSHandler	Overwrite the respective functionality for necessary security primitives: authenticated encryption, key agreement, pseudorandom generator, and secret sharing.
Application	AppServer	Overwrite <code>use_output()</code> to specify how the server uses the output of distributed DP.
	AppClient	Overwrite <code>prepare_data()</code> and <code>use_output()</code> to specify how a client prepares the input and consumes the output of distributed DP, respectively.

distributed DP algorithms by leveraging the generic programming interface offered by Hyades. Specifically, Table 4 shows the base classes that are ready for customization.

The first base class, ProtocolServer, can be instantiated to implement different *server-end workflow* (like the one listed in Table 2). To help developers focus on developing the computation logic, Hyades provides them with established communication primitives (that are based on Socket . IO [6]) to which they can delegate the server-client interactions. For ease of specifying the execution order and resource dependencies of different operations, Hyades further provides the `set_graph_dict()` method where developers can annotate to help Hyades plan the optimal pipeline acceleration (§5.2). Similarly, for implementing *client-end workflow*, Hyades supplies developers with the base class Protocol Client to customize. Also, Hyades provides the method `set_routine()` for developers to specify which part of the client workflow is triggered by a specific server request.

Apart from the high-level workflow construction, Hyades also provides developers with generic base classes to implement their own *privacy and security primitives*, including but not limited to differential privacy mechanisms (DPHandler), authenticated encryption schemes (AEHandler), key agreement protocols (KAHandler), pseudorandom number generators (PGHandler), and secret sharing algorithms (SSHandler). This enables developers to easily plug in and experiment with diverse privacy and security building blocks.

Support for Diverse Applications. As indicated in Table 4, Hyades also enables developers to readily port the aggregation framework to fuel other privacy-sensitive applications beyond FL. Specifically, developers can inherit the AppServer class with the `use_output()` method overwritten to specify how the aggregated result is consumed by the server. Similarly, they can also instantiate their own AppClient with 1) the method `prepare_data()` overwritten to define how a client’s data is produced, as well as 2) the method `use_output()` to configure how the aggregated result is consumed by the client. We will open-source Hyades and hereby invite the community to contribute more to privacy-preserving data analytics research.